Selected Papers of The Society of Naval Architects of Korea, Vol. 1, No.1, 1993, pp. 76~90.

Development of KD-Propeller Series Using a New Blade Section

Jin-Tae Lee*, Moon-Chan Kim*, Jong-Woo Ahn* and Ho-Chung Kim**

(From T.S.N.A.K., Vol.28, No.2, 1991)

Abstract

A new propeller series is developed using the newly developed blade section(KH18 section) which has better cavitation characteristics and higher lift-drag ratio at wide angle-of-attack range than a conventional section.

The radial pitch distribution of the new series propellers is variable since they were designed adaptively to a typical wake distribution. Basic geometric particulars of the series propellers, such as chord length, thickness, skew and rake distributions, are determined on the basis of recent full scale propeller geometric data. The series is developed for propellers having 4 blades, and blade area ratios of 0.3, 0.45, 0.6 and 0.75. Mean pitch ratios are varied as 0.5, 0.65, 0.8, 0.95 and 1.1 for each blade area ratio. The new propeller series consists of 20 propellers and is named as the KD(KRISO-DAEWOO)-propeller series.

Propeller open-water tests are performed at the towing tank, and cavitation observation tests and fluctuating pressure tests are carried out at the cavitation tunnel of KRISO. $B_P-\delta$ curves, which can be used to select the optimum propeller diameter at the preliminary design stage, are derived from a regression analysis of the propeller open-water test results.

The KD-cavitation chart is derived from the cavitation observation test results by choosing the local maximum lift coefficient and the local cavitation number as parameters. The cavity extent predicted by the KD-cavitation chart would be more accurate compared to that by an existing cavitation charts, such as the Burrill's cavitation chart, since the former is derived from the cavitation observation test results in a typical ship's wake, while the latter is derived from the test results in a uniform flow.

1. Introduction

The design procedure of marine propeller consists of the preliminary design stage, the detail design stage and the performance analysis stage. At the preliminary design stage, principal geometric characteristics of the propeller, such as the optimum propeller diameter, expanded blade area rat-

* Member, Korea Research Institute of Ships and Ocean Engineering
** Member, Daewoo Shipbuilding & Heavy Machinery

io and pitch ratio, are selected with the given design data using a methodical propeller series. The methodical series data are collections of experimental data of propellers whose geometries are systematically varied.

At the detail design stage, the radial pitch and camber distributions are determined, using a lifting line theory and a lifting surface theory, to match the desired radial and chordwise loading shapes. At the performance analysis stage, off-design-point performances, unsteady propeller forces in a nonuniform wake field and cavitation characteristics at the behind condition, are calculated using performance analysis programs with the designed propeller geometry. The final propeller geometry is usually confirmed through model tests.

Even though the detail design becomes faster and more accurate due to the availability of large and fast computers and newly developed computer codes, accurate selection of principal geometry of the propeller at the preliminary design stage is still important. It not only reduces the number of iterations in the design process and model test, but also determines the important geometric characteristics of the final propeller. Accurate and prompt prediction of propeller performance is especially important at the contract design stage, when various design parameters are extensively varied during the initial trade-off studies.

As the propeller design with the newly developed blade section(KH18 section) becomes popular[1,2], a new propeller series having the KH18 section is needed. Adaptation of the KH18 blade section, especially for high speed container ship propellers,
is increasing, because the new blade section gives better cavitation characteristics at wide angle-of-attack range[3,4].

In this paper procedures for the development of the new propeller series, are described. The new series propellers are equipped with the KH18 section, and have radially varying pitch distribution. Geometries of the new series propellers, such as chord length, thickness, skew and rake distributions, are selected from recent full scale propeller geometric data, so that the initial performance prediction using the new propeller series can be more realistic. The new series is named as the KD(KRISO-DAEWOO)-propeller series.

2. Design of series propellers

Radial pitch distribution of existing series propellers, such as B-series and MAU-series, is generally uniform, while a realistic propeller designed adaptively to a ship's wake distribution has a radially varying pitch distribution. In order to design a realistic propeller at the preliminary design stag e, a propeller series of which pitch distribution is radially varying is needed. The pitch distributions of the KD-series propellers are radially varying because they are designed adaptively to a typical wake distribution. The circumferential averaged input effective wake is shown in Fig. 2, which is predicted from a typical nominal wake of a container ship.

Basic geometric particulars, such as chord length, thickness, skew and rake distributions, are determined on the basis of recent full scale propeller data[5]. The KD-series propellers are designed with the KH18 blade section which shows better cavitation characteristics and high lift-drag ratio at wide angle-of-attack range.

The propeller design method using the KH18 blade section is the same as the design method using a conventional section, except that the most suitable chordwise loading shape is not known a priori. In the proposed propeller design method, three kinds of chordwise loading shapes (A−, B− and C-types in Fig. 1) are tested[4].

The A-type has less loading near the leading edge so that the negative pressure peak value at the leading edge near the wake peak region decrease. The cavity inception speed of the propeller with the A-type loading is expected to increase and the cavity extent is expected to de-

Table 1 Basic geometric data for the KP 197 propeller

Propeller No.	KP 197	Propeller Name	KP 197
Designed by	KRISO	Ship Name	CONTAINER
Propeller Type	FPP	No. of Propeller	SINGLE
Diam.(Model)	254.902mm	Scale Ratio(λ)	30.600
A_E/A_O	.5515	$(P/D)_{mean}$	.9810
Skew(°)	24.86	Rake(°)	.00
Section Type	KH18	Hub Ratio	.1800
No. of Blades	4	Comment	A+C Type

r/R	P/D	X_m/D	θ_m(°)	C/D	$f_o/D(10^3)$	$t_o/D(10^3)$	f_o/C
.20	.6201	.0000	−1.92	.2069	12.68	46.00	.0613
.25	.6891	.0000	−3.37	.2234	12.42	42.40	.0556
.30	.7544	.0000	−4.27	.2389	11.87	38.90	.0497
.40	.8804	.0000	−4.56	.2684	10.68	32.29	0.398
.50	.9668	.0000	−3.10	.2948	9.52	26.00	.0323
.60	1.0130	.0000	−.18	.3150	8.38	20.29	.0266
.70	1.0366	.0000	3.92	.3213	6.94	15.50	.0216
.80	1.0381	.0000	8.89	.3007	5.38	11.00	.0179
.90	1.0314	.0000	14.45	.2342	3.61	6.90	.0154
.95	1.0251	.0000	17.36	.1757	2.60	5.00	.0148
1.00	1.0173	.0000	20.30	.0000	.00	3.21	.0000

Table 2 Design points for the KD-series propellers

P/D	A_E/A_O	0.30	0.45	0.60	0.75
0.50	J	0.233	0.203	0.173	0.143
	K_T	0.1312	0.1559	0.1717	0.1840
0.65	J	0.444	0.414	0.384	0.354
	K_T	0.1251	0.1532	0.1722	0.1882
0.80	J	0.625	0.595	0.565	0.535
	K_T	0.1231	0.1527	0.1730	0.1904
0.95	J	0.778	0.748	0.718	0.688
	K_T	0.1288	0.1596	0.1820	0.2013
1.10	J	0.905	0.875	0.845	0.815
	K_T	0.1418	0.1762	0.1999	0.2197

Table 3 Geometric characteristics of the KD-series propellers

r/R	$\frac{P(r)^*}{D}$	$\frac{f_o(r)^{**}}{c(r)}$	$\frac{c(r)}{DA_E/A_O}$	$\frac{t_o(r)^{***}}{c(r)}$	θ_{mi}(°)
0.20	0.6005	1.0000	0.3763	1.1832	−1.921
0.25	0.6673	0.9057	0.4103	1.0000	−3.369
0.30	0.7306	0.8098	0.4407	0.8545	−4.267
0.40	0.8526	0.6498	0.4948	0.6321	−4.560
0.50	0.9362	0.5269	0.5387	0.4673	−3.103
0.60	0.9810	0.4343	0.5638	0.3484	−0.179
0.70	1.0010	0.3519	0.5638	0.2660	3.916
0.80	1.0053	0.2912	0.5325	0.1999	8.899
0.90	0.9988	0.2508	0.4402	0.1517	14.448
0.95	0.9927	0.2407	0.3372	0.1435	17.356
1.00	0.9852	−	0.0000	−	20.300

crease, while the cavity behavior can be easily unstable and the possibility of propeller erosion may increase.

The C-type has more loading near the leading edge. The propeller with this type loading would have a lower cavity inception speed and a larger extent of cavity than the propeller with the A-type loading, but cavity behavior would be stable. The most suitable chordwise loading shape should be determined by considering operation conditions of a propeller.

The KP197 propeller, which is equipped with

$$* \; P(r)/D = \frac{(P/D)_{mean}}{0.95} P(r)/D^* + (0.43(P/D)_{mean} - 0.95)\left(\frac{r}{R} - 0.683\right) - 0.30(A_E/A_O - 0.6)\left(\frac{r}{R} - 0.683\right)$$

$$** \; f_o(r)/c(r) = f_o(r)/c(r)^{**}(0.165(P/D)_{mean} + 0.4358)/5.932 \cdot (0.2341(A_E/A_O)^2 - 0.4013(A_E/A_O) + 0.7493)$$

$$*** \; t_o(r)/c(r)^{***} \cdot (0.3756(A_E/A_O)^2 - 0.685(A_E/A_O) + 0.448)$$

the KH18 blade section, is designed to have the A-type loading at the inner radii and the C-type loading at the outer radii of 0.7 propeller radius. This combination of loading shape is proven to give satisfactory cavitation characteristics through the full scale application of the KP197 propeller for a container ship. Geometric data of the KP197 propeller, which is selected as a parent propeller of the KD-series, are shown in Table 1.

The KD-series is developed for 4 bladed propellers. Model propellers for the development of the series consist of 20 propellers and are given the model propeller numbers from KP201 to KP220. The propellers have blade area ratios of 0.3, 0.45, 0.6, 0.75, and have mean pitch ratios of 0.5, 0.65, 0.8, 0.95, 1.1 for each blade area ratio, respectively.

Design points of the series propellers are selected as shown in Table 2 considering the operation conditions of existing series propellers. Geometries of the KD-series propellers are systemically varied from the reference geometry of the KP214 propeller($A_E/A_O=0.6$, $P/D=0.95$) which has been designed after the geometry of the KP197 propeller. Basic geometric characteristics of the KD-series propellers are shown in Table 3 and Fig. 3. The radial loading distributions of the KD series propellers are controlled to have the standard loading shape of the KP197 as shown in Figs. 4 and 5. The chordwise loading shapes of

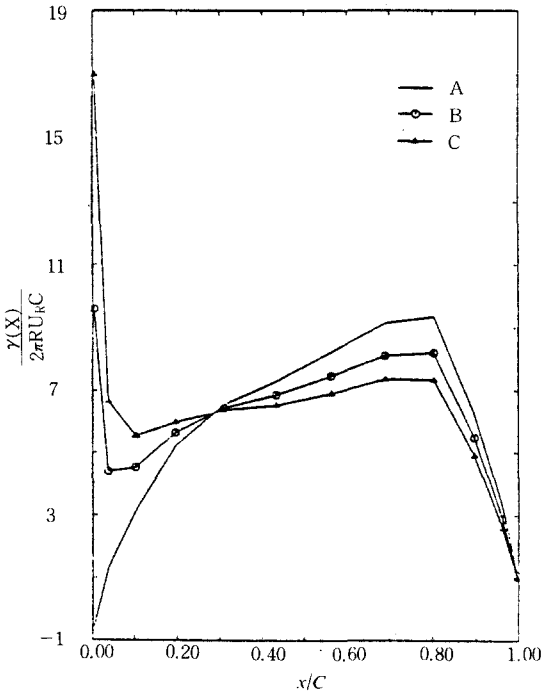

Fig. 1 Comparison of the chordwise loading types

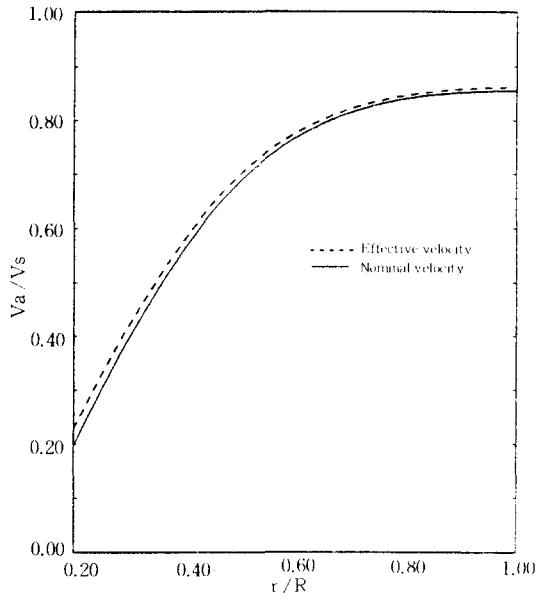

Fig. 2 Prediction of the circumferential mean effective velocity distribution

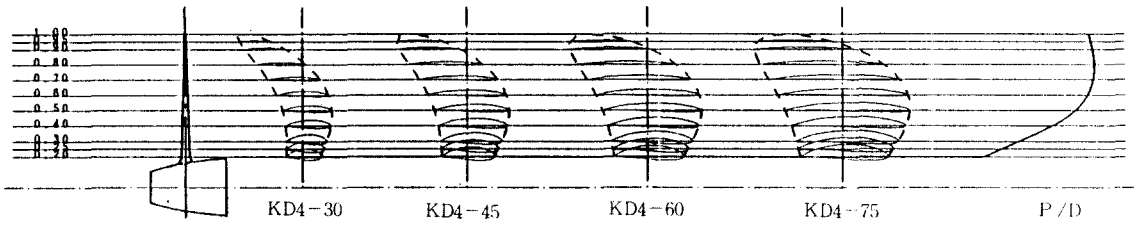

Fig. 3 General plan of KD-propeller series

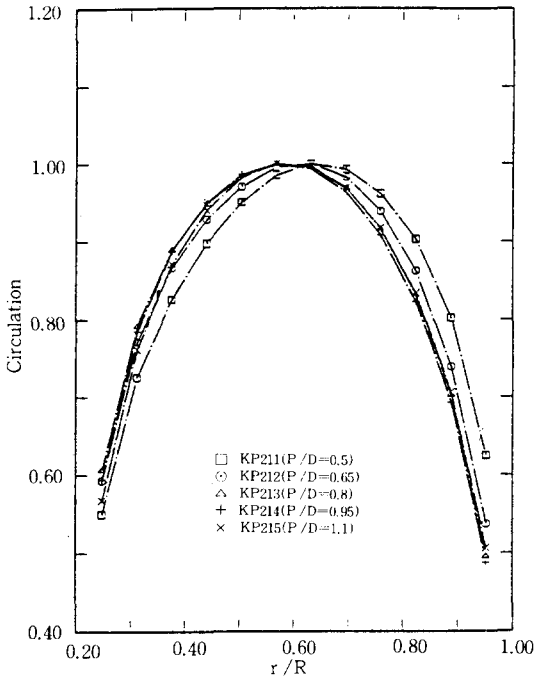

Fig. 4 Radial circulation distributions of the different pitch propellers having the same blade area ratio(A_E/A_O=0.6)

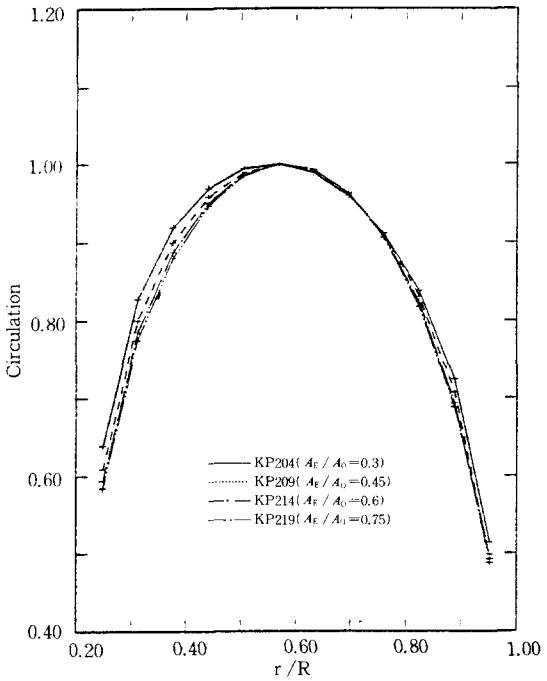

Fig. 5 Radial circulation distributions of the different blade area ratio propellers having the same mean pitch(P/D=0.95)

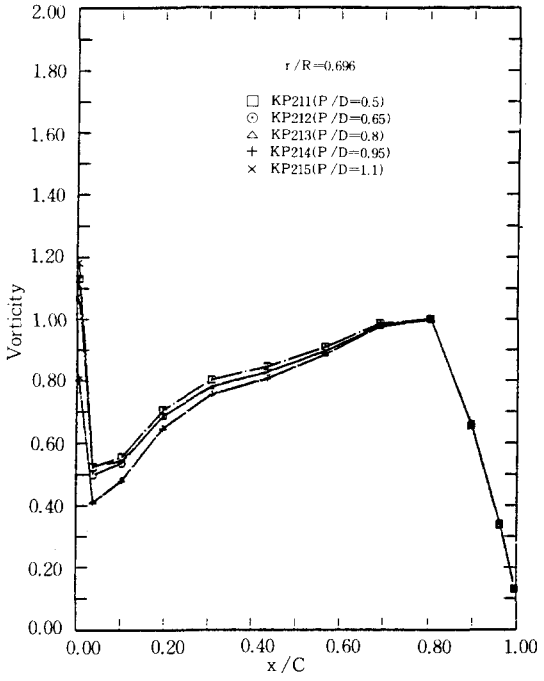

Fig. 6 Chordwise loading distributions at r/R= 0.696 of the different pitch propellers having the same blade area ratio(A_E/A_O=0.6)

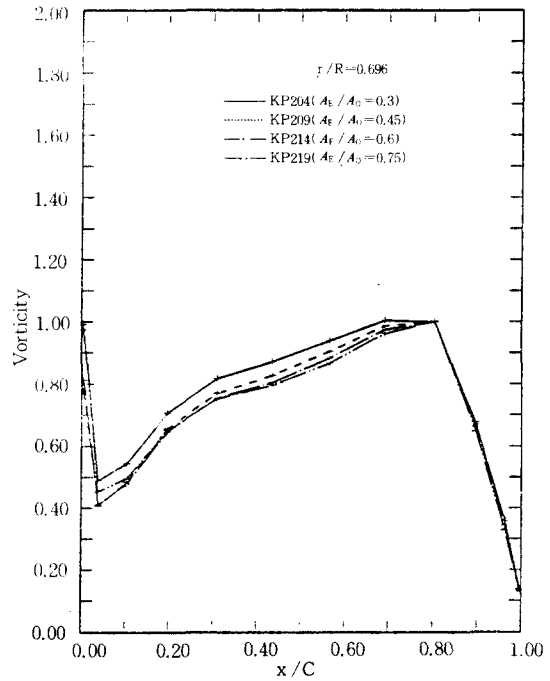

Fig. 7 Chordwise circulation distributions at r/R= 0.696 of the different blade area ratio propellers having the same mean pitch(P/D=0.95)

the typical KD-series propellers at 0.7 propeller radius are shown in Figs. 6 and7.

The KH18 section is adopted as the blade section of the KD-series propellers except the tip region (outer radii of 0. 95R), where the KH21 section is adopted. The KH21 section has the same camber distribution as the KH18 section, but its thickness distribution is elliptic near the leading edge region. The maximum thickness point is located on the mid-chord, in order to stabilize the sheet cavities near the tip region.

Application of the KD-propeller series at the preliminary design stage would provide a more realistic propeller geometry and more accurate performance prediction, provided that the wake distribution of the ship is not so different from the selected input wake. The KD-propeller series is expected to reduce the number of iterations in finalizing the propeller geometry through the detail design and model test.

3. Model test of the series propeller

Propeller open-water tests are performed at the towing tank, and cavitation observation tests and fluctuating pressure tests are carried out at the cavitation tunnel of KRISO. The propeller open-water test is to measure the thrust and torque acting on the propeller for varying advance coefficient ($J_a = \frac{V_a}{nD}$).

Dependance of the open-water test results on the variation of Reynolds number is investigated with eight propellers which have the highest and lowest pitch ratios in the four blade area ratio group. It is concluded from the Reynolds number variation tests that propeller open-water tests in the towing tank should be performed at Reynolds number higher than 5×10^5.

Cavitation observation tests are performed in a wire-mesh generated wake as shown in Fig. 8, which is a typical wake distribution for a container ship. Thrust identity conditions are matched for the realization of test conditions and the tunnel pressure is adjusted to match the cavitation number. Cavitation behavior, extent and occurrence range are sketched during the cavitation observation tests.

Since the pitch ratios of the series propellers vary from 0.5 to 1.1, flow speed in the cavitation tunnel during the cavitation observation tests also varies in order to match the test condition. It is investigated whether the wake distribution shape changes according to the change of tunnel flow velocity. Comparison of the wake distribution in the circumferential direction for tunnel flow speeds of 2.5m/s and 4.5m/s is shown in Fig. 9, where two wake distributions are practically identical. In order to prevent the deformation of the wake screen during the cavitation tests, a brass tube is installed to support the wake screen at the shaft center position.

Fluctuating pressure test is to measure the fluctuating pressure induced by the propeller on the flat plate located above the propeller, where five pressure transducers are mounted. The tip clear-

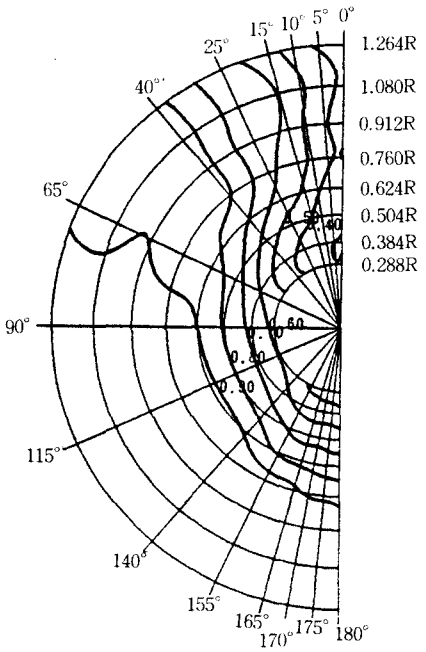

Fig. 8 Iso-axial velocity curves of the simulated wake at 4.5m/s

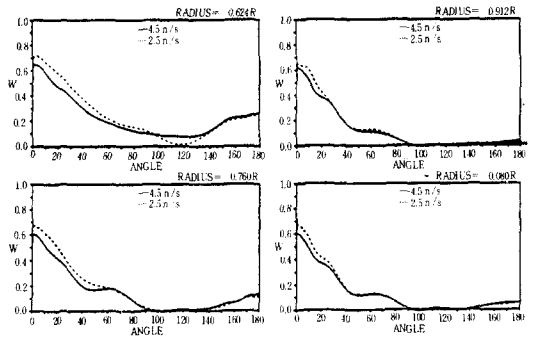

Fig. 9 Comparison of the wake distribution in circumferential direction measured at 2.5m/s with that at 4.5m/s

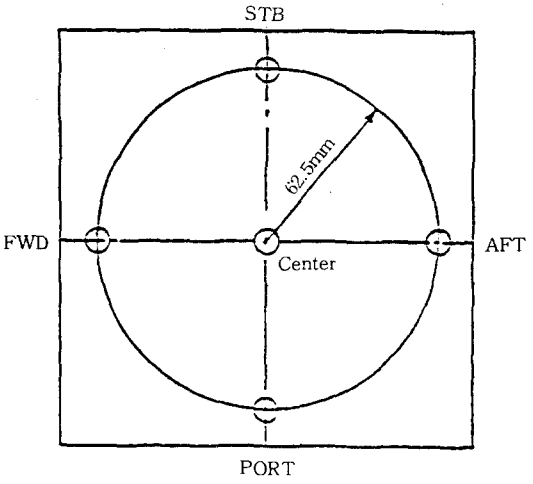

Fig. 10 Positions of 5 pressure transducers on the flat plate

ance between the plate and the blade tip at upright position is 7.16cm (28.6% of the propeller diameter). The pressure measurement positions on the plate is shown in Fig. 10. Test conditions are selected as the conditions of the cavitation observation test. The measured fluctuating pressure values are analyzed using an FFT analyzer. The fluctuating pressure of a full-scale ship is predicted with the analysis results up to the 4-th blade harmonics.

The cavitation observation tests and fluctuating pressure tests are carried out simultaneously.

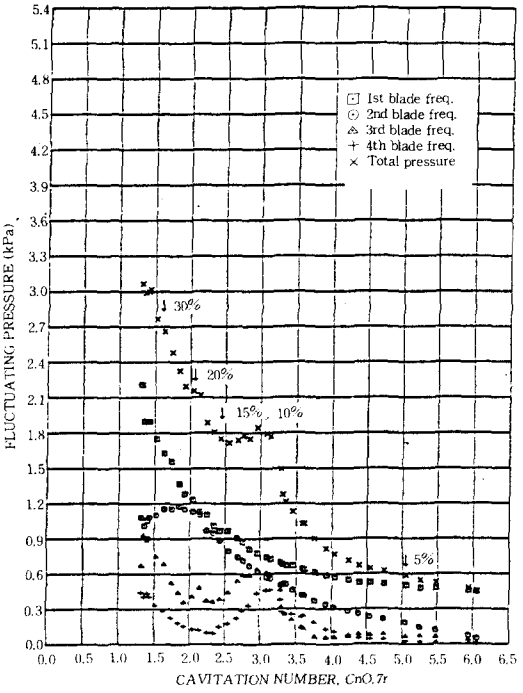

Fig. 11 Fluctuating pressure values as a function of cavitation number (KP214 propeller, 25rps)

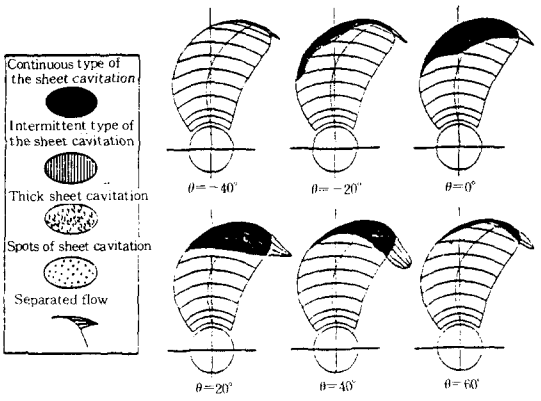

Fig. 12 Sketches of the cavitation pattern for the KP214 propeller

The three operating thrust coefficients($K_T = \frac{T}{\rho n^2 D^4}$) are selected for each propeller, and tunnel pressure is adjusted for 2~3 cavitation numbers at each operating thrust coefficients, as shown in Table 4.

Table 4 Summary of test conditions and maximum fluctuating pressure values at the center pressure transducer

No.	K_T (C_l^{max})	Cavitating area	σ_o	Max. Fluct. Press. at Center	No.	K_T (C_l^{max})	Cavitating area	σ_c	Max. Fluct. Press. at Center
KP201	0.142 (0.172)	5%	0.643	0.410	KP206	0.148 (0.127)	5%	0.457	0.824
		10%	0.439	1.100			10%	0.303	2.251
		20%	0.220	2.048			20%	0.199	2.997
	0.131 (0.174)	5%	0.650	0.346		0.133 (0.127)	5%	0.455	0.661
		10%	0.426	1.014			10%	0.296	1.803
		20%	–	–			20%	0.154	2.078
	0.107 (0.171)	5%	0.596	0.316		0.098 (0.120)	5%	0.308	1.803
		10%	0.376	1.049			10%	0.202	0.661
		20%	–	–			20%	–	–
KP202	0.148 (0.225)	5%	0.845	0.297	KP207	0.156 (0.165)	5%	0.619	0.472
		10%	0.522	1.032			10%	0.394	1.253
		20%	0.325	1.889			20%	0.225	2.024
	0.130 (0.217)	5%	0.645	0.358		0.135 (0.159)	5%	0.430	0.779
		10%	0.459	0.922			10%	0.338	1.356
		20%	0.208	1.920			20%	0.218	2.235
	0.111 (0.209)	5%	–	–		0.103 (0.149)	5%	0.374	0.609
		10%	0.452	0.386			10%	0.251	1.236
		20%	0.263	1.600			20%	–	–
KP203	0.156 (0.263)	5%	–	–	KP208	0.181 (0.197)	5%	0.793	0.361
		10%	0.717	0.295			10%	0.490	0.905
		20%	0.536	0.810			20%	0.323	1.885
	0.130 (0.250)	5%	–	–		0.159 (0.189)	5%	0.775	0.368
		10%	0.609	0.346			10%	0.396	1.384
		20%	0.433	1.103			20%	0.280	2.039
	0.111 (0.239)	5%	0.757	0.272		0.142 (0.183)	5%	0.575	0.385
		10%	0.567	0.439			10%	0.379	1.346
		20%	0.403	1.166			20%	0.283	1.973
KP204	0.161 (0.294)	5%	–	–	KP209	0.208 (0.229)	5%	0.938	0.508
		10%	0.922	0.432			10%	0.668	0.795
		20%	0.645	0.722			20%	0.459	1.489
	0.139 (0.281)	5%	–	–		0.163 (0.211)	5%	0.724	0.537
		10%	0.856	0.424			10%	0.563	0.864
		20%	0.606	0.740			20%	0.417	1.280
	0.114 (0.266)	5%	–	–		0.141 (0.203)	5%	0.699	0.489
		10%	0.739	0.433			10%	0.532	0.769
		20%	0.495	1.060			20%	0.357	1.534
KP205	0.178 (0.325)	5%	–	–	KP210	0.208 (0.245)	5%	–	–
		10%	1.105	0.587			10%	0.787	1.664
		20%	0.789	0.674			20%	0.534	1.173
	0.139 (0.301)	5%	–	–		0.162 (0.226)	5%	–	–
		10%	0.926	0.446			10%	0.653	0.759
		20%	0.652	0.941			20%	0.439	1.665
		5%	–	–			5%	–	–
		10%	–	–			10%	–	–
		20%	–	–			20%	–	–

No.	K_T (C_T^{max})	Cavitating area	σ_v	Max. Fluct. Press. at Center	No.	K_T (C_T^{max})	Cavitating area	σ_v	Max. Fluct. Press. at Center
KP211	0.156 (0.097)	5%	0.371	0.795	KP216	0.160 (0.079)	5%	0.248	2.149
		10%	0.212	2.386			10%	0.184	2.886
		20%	0.120	2.018			20%	–	–
	0.142 (0.098)	5%	0.320	1.073		0.145 (0.080)	5%	0.280	1.458
		10%	0.198	2.518			10%	0.165	2.984
		20%	0.112	2.201			20%	–	–
	0.103 (0.095)	5%	0.186	1.826		0.103 (0.077)	5%	0.206	1.319
		10%	–	–			10%	0.123	2.819
		20%	0.109	3.180			20%	–	–
KP212	0.185 (0.133)	5%	0.656	0.459	KP217	0.210 (0.110)	5%	0.488	0.838
		10%	0.353	1.973			10%	0.279	2.623
		20%	0.209	2.252			20%	0.161	2.224
	0.154 (0.128)	5%	0.453	0.682		0.181 (0.108)	5%	0.432	0.811
		10%	0.267	2.253			10%	0.253	2.934
		20%	0.171	2.854			20%	0.112	3.130
	0.116 (0.119)	5%	0.244	1.411		0.155 (0.104)	5%	0.348	1.328
		10%	0.191	2.260			10%	0.200	3.265
		20%	–	–			20%	0.117	3.830
KP213	0.212 (0.161)	5%	0.690	0.541	KP218	0.214 (0.132)	5%	0.551	0.703
		10%	0.436	2.354			10%	0.359	3.021
		20%	0.287	2.153			20%	0.208	2.882
	0.184 (0.154)	5%	0.503	0.726		0.186 (0.126)	5%	0.472	0.966
		10%	0.348	1.662			10%	0.273	2.962
		20%	0.247	2.727			20%	0.180	3.196
	0.156 (0.147)	5%	0.481	0.613		0.152 (0.120)	5%	0.404	0.772
		10%	0.309	1.663			10%	0.241	2.462
		20%	0.207	3.156			20%	0.148	3.758
KP214	0.240 (0.186)	5%	0.769	0.617	KP219	0.230 (0.149)	5%	0.595	0.785
		10%	0.497	1.948			10%	0.457	1.919
		20%	0.319	2.260			20%	0.261	2.513
	0.203 (0.176)	5%	0.740	0.574		0.184 (0.139)	5%	0.548	0.780
		10%	0.467	1.520			10%	0.371	2.482
		20%	0.302	2.138			20%	0.215	3.498
	0.169 (0.166)	5%	0.653	0.563		0.161 (0.134)	5%	0.577	0.703
		10%	0.432	1.391			10%	0.352	2.387
		20%	0.296	2.380			20%	0.214	3.356
KP215	0.266 (0.208)	5%	1.025	0.679	KP220	0.224 (0.158)	5%	0.681	0.905
		10%	0.729	1.038			10%	0.482	1.960
		20%	0.453	2.120			20%	0.317	2.220
	0.220 (0.193)	5%	0.851	0.720		0.172 (0.147)	5%	0.564	0.839
		10%	0.690	0.819			10%	0.414	2.009
		20%	0.383	2.060			20%	0.272	2.837
	0.173 (0.179)	5%	0.660	0.818			5%	–	–
		10%	0.526	1.358			10%	–	–
		20%	0.341	2.380			20%	–	–

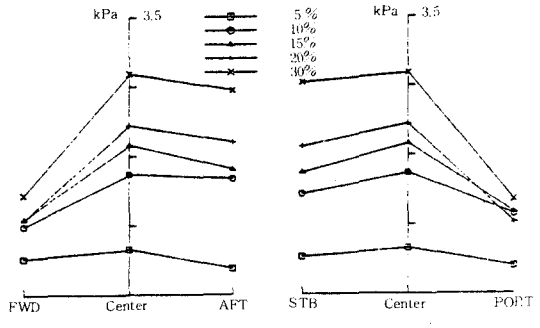

Fig. 13 Distribution of fluctuating pressures on the flat plate according to cavitation extent variation for the KP214 propeller in $J_s=0.68$

Fluctuating pressure values are measured while the cavitation number is lowered continuously for the KP214 propeller at the operating condition of $K_T=0.203$. As shown in Fig. 11, the fluctuation pressure values increase as the cavitation number decreases. But there is a deflection point when the maximum cavity extent becomes 10% of the blade area. The cavitation behaviour is observed as unstable and the higher blade harmonic values of the measured pressure at this test condition become large. A typical sketch of the cavitation observation test and the measured fluctuating pressure distribution on the flat plate are shown in Fig. 12 and Fig. 13, respectively. Summary of fluctuating pressure tests for the KD-series propellers operating at various test conditions is given in Table 4.

4. Regression analysis of model test results and derivation of the KD-cavitation chart

The model test results are systematically rearranged so that the propeller series charts can be derived. These series charts enable us to predict more accurate preliminary design and performance. In this research, the $B_P-\delta$ curves and the cavitation prediction curves are derived, which are named as the KD-series chart and the KD-cavitation chart, respectively.

In order to derive the regression formula for the propeller open-water test results, a statistical regression analysis method using simple high-order polynomials is adopted. The thrust and torque coefficients are expressed as 11th order polynomials of advanced ratio(J) and pitch ratio (P/D), as shown in the following equations. These equations are defined for the group of propellers having the same blade number and the same blade area ratio.

$$K_T=\Sigma\Sigma C_{ij}^{T}(J)^i(P/D)^j$$
$$10K_Q=\Sigma\Sigma C_{ij}^{Q}(J)^i(P/D)^j$$

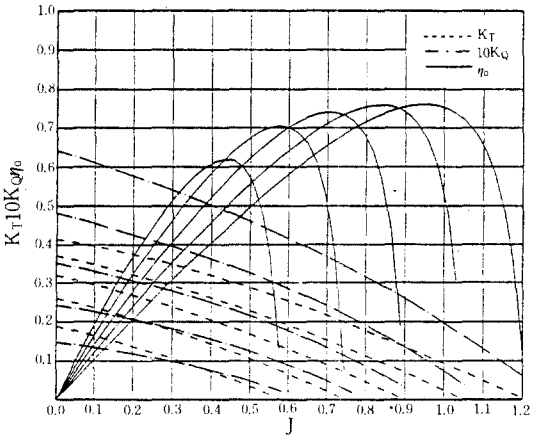

Fig. 14 Regression analysis results of the propeller open water characteristics for KD4-30

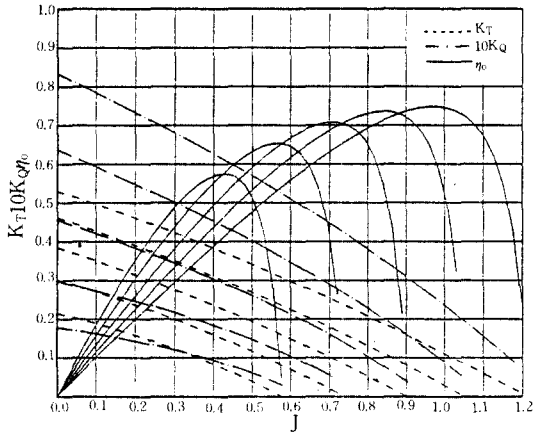

Fig. 15 Regression analysis results of the propeller open water characteristics for KD4-45

In this research, C_{ij}^{T} and C_{ij}^{Q} for the KD-series propellers are calculated from the propeller open-water test results using a least square method[6]. Using these coefficients, the propeller open water curves are generated as shown in Figs. 14, 15, 16, 17. Its application range is shown in Table 5. The $B_P-\delta$ curves are very useful to determine the optimum diameter or efficiency in the preliminary

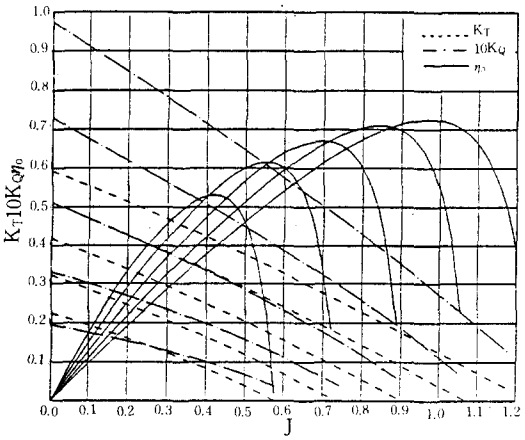

Fig. 16 Regression analysis results of the propeller open water characteristics for KD4-60

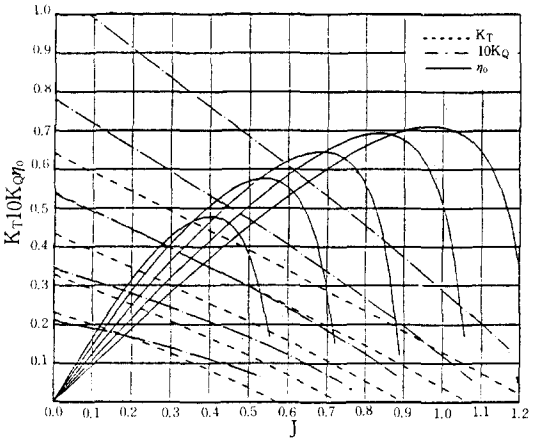

Fig. 17 Regression analysis results of the propeller open water characteristics for KD4-75

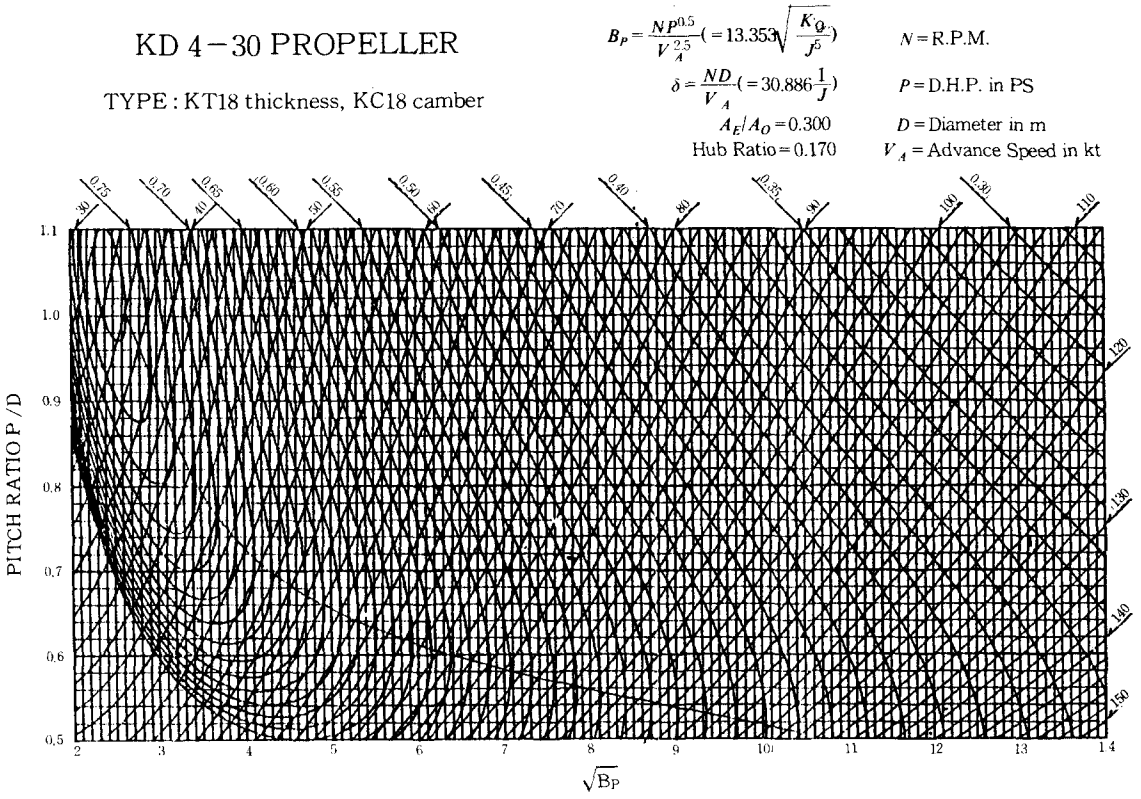

Fig. 18 $B_P-\delta$ curve for KD 4-30 propeller

KD 4−45 PROPELLER

TYPE : KT18 thickness, KC18 camber

$B_P = \frac{NP^{0.5}}{V_A^{2.5}} \left(= 13.353\sqrt{\frac{K_Q}{J^5}}\right)$ N = R.P.M.

$\delta = \frac{ND}{V_A} \left(= 30.886\frac{1}{J}\right)$ P = D.H.P. in PS

$A_E/A_O = 0.450$ D = Diameter in m

Hub Ratio = 0.170 V_A = Advance Speed in kt

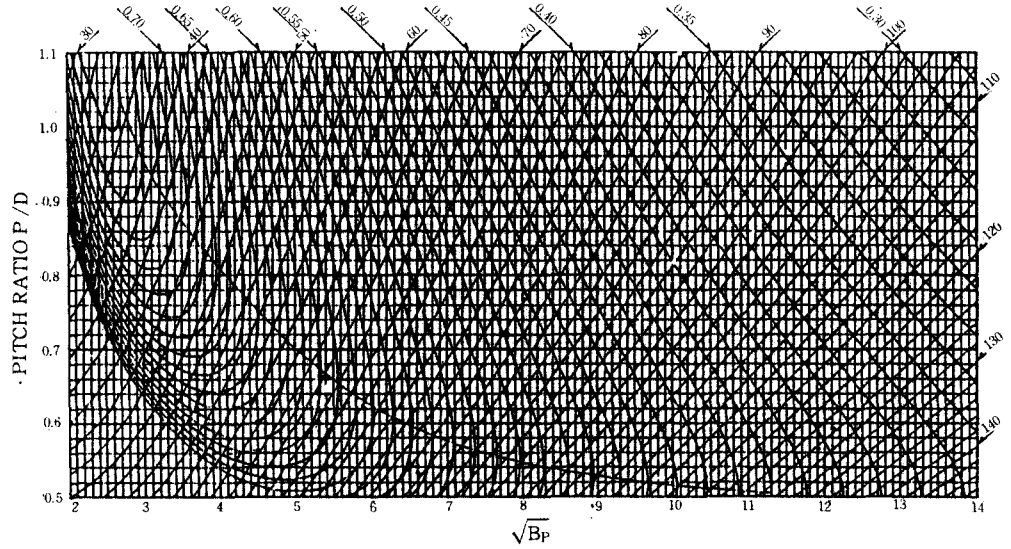

Fig. 19 $B_P-\delta$ curve for KD 4-45 propeller

KD 4−60 PROPELLER

TYPE : KT18 thickness, KC18 camber

$B_P = \frac{NP^{0.5}}{V_A^{2.5}} \left(= 13.353\sqrt{\frac{K_Q}{J^5}}\right)$ N = R.P.M.

$\delta = \frac{ND}{V_A} \left(= 30.886\frac{1}{J}\right)$ P = D.H.P. in PS

$A_E/A_O = 0.600$ D = Diameter in m

Hub Ratio = 0.170 V_A = Advance Speed in kt

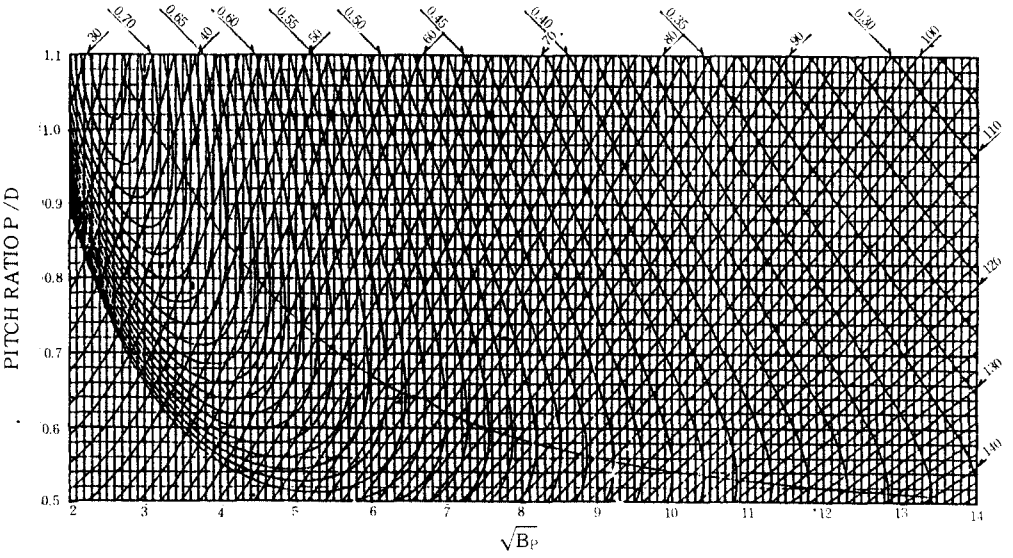

Fig. 20 $B_P-\delta$ curve for KD 4-60 propeller

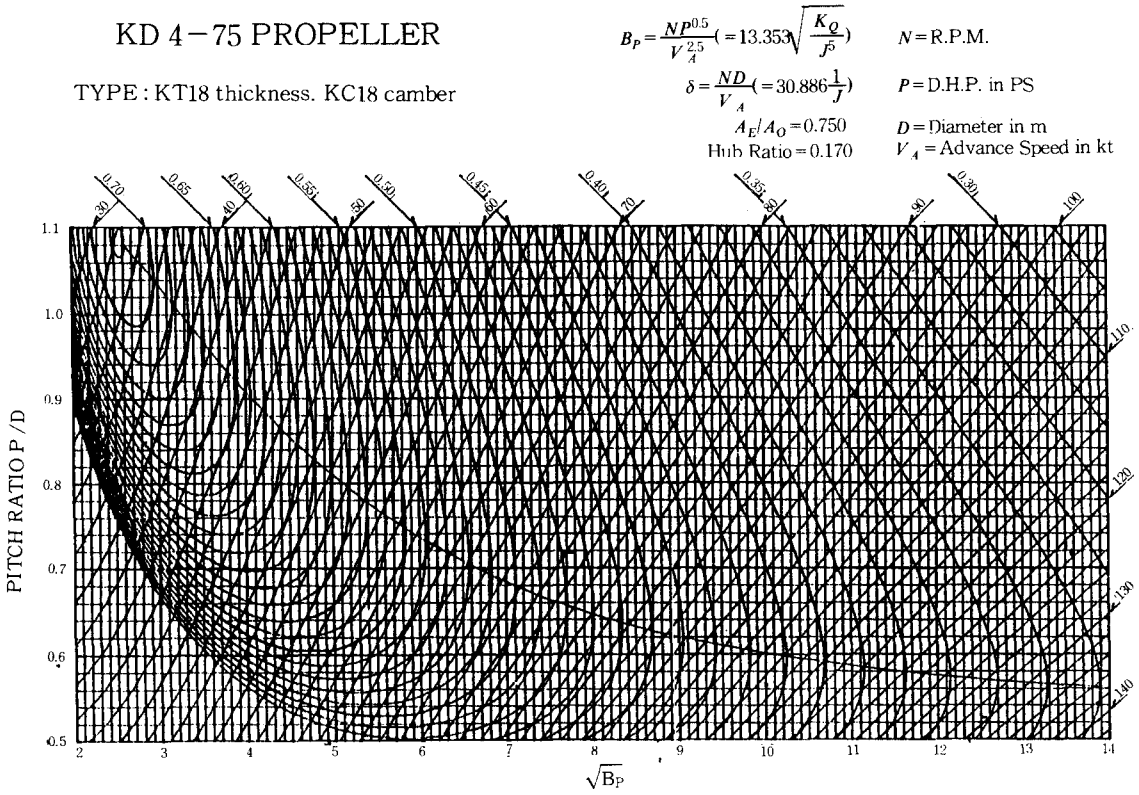

Fig. 21 $B_P-\delta$ curve for KD 4-75 propeller

Table 5 Application range of the regression formula for the KD−propeller series

Z	A_E/A_O	Name	P/D
4	0.30	KD 4-30	0.50~1.10
	0.45	KD 4-45	0.50~1.10
	0.60	KD 4-60	0.50~1.10
	0.75	KD 4-75	0.50~1.10

design stage with minimum design parameters (delivered horsepower P_D, rotation speed N, propeller advanced velocity V_A). The $B_P-\delta$ curves are shown in Figs. 18, 19, 20, 21. The y-axis represents Taylor's power coefficient ($B_P=\frac{NP^{0.5}}{V_A^{2.5}}=13.353\sqrt{\frac{K_Q}{J}}$) and the x-axis Taylor's advanced coefficient ($\delta=\frac{ND}{V_A}=30.886\frac{1}{J}$), respectively.

Existing cavitation charts, such as the Burrill's cavitation chart, do not accurately predict cavitation extent on propeller blade surfaces because those are derived from

the test results in uniform flow conditions. In the Burrill's cavitation chart, the propeller thrust loading coefficient ($\tau_c=\frac{T/A_P}{\frac{1}{2}\rho V_{0.7R}^2}$) is introduced as a loading factor, but in the KD-cavitation chart, τ_c can not be used, because the KD-series propellers are tested in a nonuniform wake field.

The maximum local lift coefficient $C_{l0.8R}^{max}$ is introduced to express the correlation between the propeller loading and the cavitation extent. $C_{l0.8R}^{max}$ is calculated by an unsteady propeller analysis code(KPD2) and is defined as

$$C_{l0.8R}^{max}=\frac{L_{max}}{\frac{1}{2}\rho U_R^2 C})0.8R=(\frac{2\Gamma_{max}}{U_R C})0.8R$$

where the calculation point is selected as 0.8 radius instead of 0.7 radius of propeller, because cavitation occurs more frequently at 0.8R than at 0.7R.

The cavitation occurring lines of 5%, 10%, 20%, 30%, are derived from the cavitation observation test results of the KD-series propellers. A typical example of the 20% cavitation occurring line is shown in Fig. 22 with the cavitation observation test results. The KD-cavitation chart is shown in Fig. 23. As mentioned before, the KD-cavitation chart would provide a more accurate cavitation prediction at preliminary stage than those by the Burrill's cavitation chart, since the former is derived using the test results in a nonuniform wake field while the latter using the test results in a uniform flow.

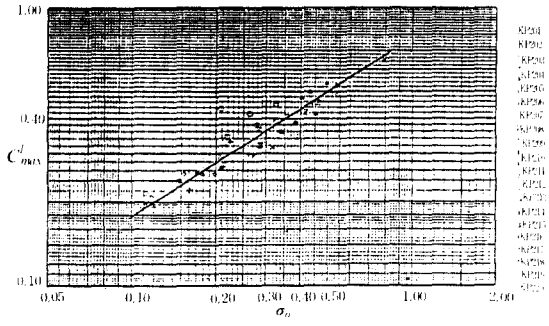

Fig. 22 Comparison of the cavitation prediction curve and cavitation model test results for the 20% cavitating area line

5. Conclusions

Procedures for the development of the KD-propeller series, which was KH18 blade section, is derived in the paper. Important conclusions can be summarized as follows :

- The KD-propeller series is developed for 4 bladed propellers. Since the KH18 blade section has better cavitation characteristics, the KD-series propellers are expected to have

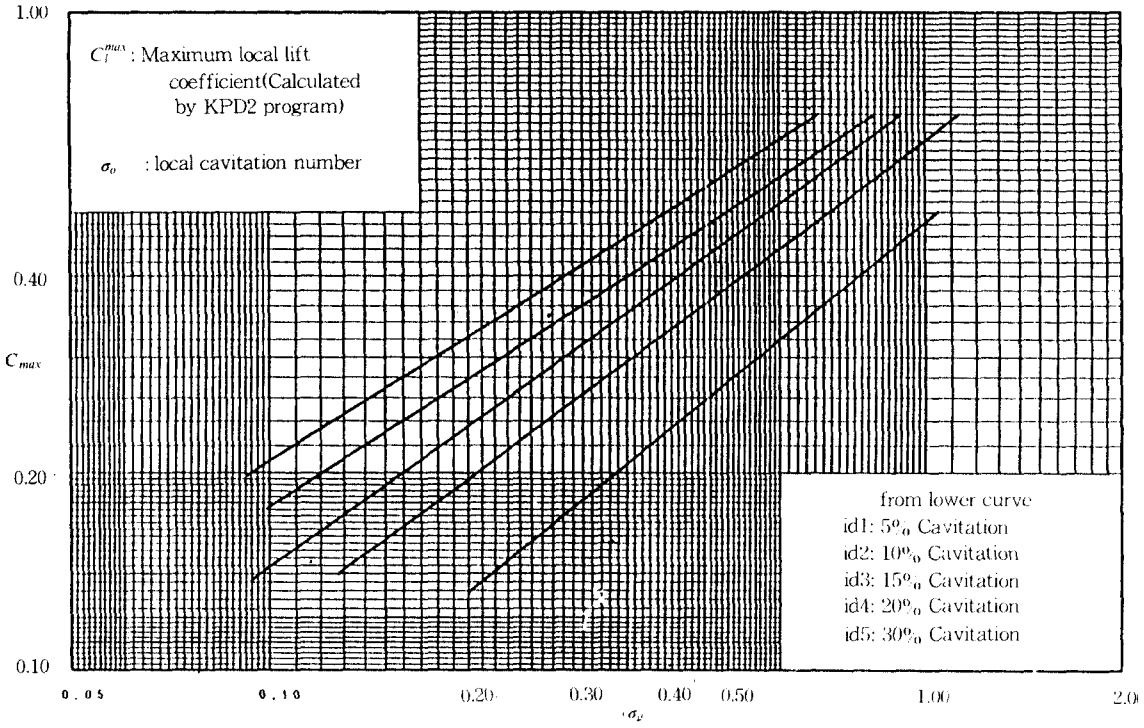

Fig. 23 The KD-cavitation chart

better cavitation performances compared to the existing series propellers.

- Geometry of the KD-series propellers is designed on the basis of recent full scale propeller geometric data. The pitch distribution is radially varying in order to be adaptive to a typical input wake. A more realistic geometry and more accurate performance prediction would be provided at the preliminary design stage, if the KD-propeller series is adopted.
- $B_P-\delta$ curves are derived from a regression analysis of the propeller open-water test results. The KD-cavitation chart is derived from the cavitation observation test results. Since the cavitation observation tests are performed in a typical ship's wake, cavity extent predicted by the KD-cavitation chart would be more accurate compared to that by an existing cavitation chart.

Acknowledgement

This research is supported partly by MOST (Ministry of Science and Technology, Korea) and Daewoo Shipbuilding & Heavy Machinery. The authors wish to acknowledge the valuable comments of Prof. Chang-Sup Lee of the Chungnam National Univ., Taejeon, Korea. Efforts of Mr. Kyung-Yuel Kim and Chang-Yong Lee to perform the numerous experimental works are thankfully acknowledged.

References

[1] Jin-Tae Lee et al., "A research on the development of KD-propeller series : Intermediate report," KRISO Report BSI584-1030 M.D, 1988. 8.

[2] Jin-Tae Lee et al., "A research on the development of KD-propeller series : Final report," KRISO Report BSI584-1030. D, 1989.

[3] Jin-Tae Lee et al., "A Propeller design method with new blade setions," *Journal of the Society of Naval Architects of Korea*, Vol. 26, No. 3, 1989.

[4] Jin-Tae Lee, Moon-Chan Kim, Jong-Woo Ahn, Ki-Sup Kim and Ho-Chung Kim, "Development of marine propellers with new blade sections for container ship," *The Propellers/Shafting '91 Symposium*, Virginia Beach, Sept. 17－18, 1991.

[5] S. Yamasaki et al., "Open-water test series with propeller models for small blade area ratio(MAU 4-30, 5-35)," *Trans. of West-Japan Society of Naval Architects*, No. 64, 1982.

[6] Moon-Chan Kim and Jin-Tae Lee, "Regression analysis of the KIMM-NACA propeller series," *Ship and Ocean Research*, Vol. 1, 1988.

[7] J.E. Kerwin and Chang-Sup Lee, "Prediction of steady and unsteady marine propeller perfomance by numerical lifting-surface theory," *SNAME* Trans. Vol. 86, 1978.